Desalination and Water Treatment
www.deswater.com

doi: 10.1080/19443994.2015.1082940

57 (2016) 16963–16969
August

Taylor & Francis
Taylor & Francis Group

Retention and separation of 4BS dye from wastewater by the N-TiO_2 ceramic membrane

Zi-bo Wang[a,*], Yu-jiang Guan[b], Bin Chen[a], Shu-li Bai[b]

[a]*College of Environmental Science and Engineering, Yangzhou University, 196 West Huayang Road, Yangzhou 225127, Jiangsu Province, China, Tel./Fax: +86 514 87978626; email: wangzb@yzu.edu.cn (Z.-b. Wang), Tel. +86 514 87978626; email: chenbinbin198711@126.com (B. Chen)*

[b]*Department of Environmental Engineering, College of Taizhou, Taizhou 318001, Zhejiang, China, Tel. +86 576 88660340; emails: guanyujiang@tzc.edu.cn (Y.-j. Guan), baishuli@tzc.edu.cn (S.-l. Bai)*

Received 30 June 2014; Accepted 10 August 2015

ABSTRACT

The aim of this work was to study the retention and separation of 4BS dye from aqueous solution using N-doped TiO_2 (N-TiO_2) ceramic membrane. An N-TiO_2 sol was synthesized by the sol–gel technique and applied to a ceramic membrane to synthesize a composite membrane. XRD analysis confirmed that the N-TiO_2 had an anatase structure. SEM images revealed that the TiO_2 particles with a diameter of 7–9 nm had been loaded on a ceramic support to form the nanoporous composites. 4BS dye containing aqueous solution was treated by the composite membranes. The operating conditions studied were the dye concentration, solution pH, the pressure and velocity of cross flow. With the coupling of photocatalysis and membrane separation, the retention rate of 99% for dye and the higher permeation flux (over 96%) were obtained. The composite membranes were found to be stable and to perform reproducibly.

Keywords: Ceramic membrane; N-doped TiO_2; Retention; 4BS dye

1. Introduction

As a highly efficient technique, membrane separation has been widely used in many fields such as petrochemical, environmental, pharmaceutical and food industries [1–4]. For dyestuff industry, nanofiltration is used as a process with applications in separation of dyestuff from wastewater. However, organic pollutants (dye) can cause severe membrane fouling, mainly as a result of pollutant adsorption onto the membrane surfaces and within the membrane pores, and the permeation flux decline and lower membrane efficiencies will occur in the membrane process [5,6]. At present, the combination of photocatalysis and membrane separation has become research hotspot. With the photocatalysis techniques, organic pollutants are degraded effectively and membrane fouling is inhibited. Moreover, the degradation products can be removed from reaction system quickly by the membrane separation techniques. At last, photocatalysis reaction is promoted due to the acceleration of mass transfer. As a result, the permeation flux is obviously increased by the coupling of photocatalysis with membrane separation.

N-TiO_2 ceramic membrane possesses the characteristic of antioxidation, acid-proof alkali and

*Corresponding author.

thermostability. In photocatalysis, membrane fouling can be cleared up effectively, and the anti-fouling properties of the ceramic membranes can be enhanced. 4BS dye is used to stain cellulose fibre like cotton, viscose rayon and linen. At present, with the coupling of photocatalysis and membrane separation, there are no reports on the N-TiO_2 ceramic membranes treating 4BS dye wastewater. Based on recycling of dye from wastewater, the composite membranes were used to separate 4BS dye from aqueous solution in this study. The optimal operating conditions, including the effects of the dye concentration, the transmembrane pressure, pH and cross-flow (CF) velocity on the separation of dye from solution, were proposed in this paper.

2. Experimental details

2.1. Materials and apparatus

Ethylenediamine, sodium hydroxide, tetrabutyl titanate, hydrochloric acid, acetic acid, absolute ethanol and all reagents used were of analytical grade. X-ray diffractometer (XRD, Bruker AXS, Germany), scanning electron microscopy (SEM, Hitachi, Japan), short-arc xenon lamp (CHF-XM-300 W, Beijing, China), electrical conductivity meter (Hana Ke Instrument Technology Co. Ltd, Beijing, China) and spectrophotometer (Cary50, U.S. Varian Technology Co. Ltd, China).

4BS dye (Tianjin Xiangrui Dye Co. Ltd, China) is soluble in water and insoluble in acetone. The dye is usually used in dyeing and printing of cellulose fibre.

2.2. Preparation of N-TiO_2 ceramic membrane

The N-TiO_2 ceramic composite membranes were synthesized by the sol–gel technique [7,8]. A mixture of absolute ethanol (15 mL), tetrabutyl titanate (15 mL), acetic acid (7 mL) and ethylenediamine (0.3 mL) was put into a beaker, and the mixture was stirred by a magnetic stirrer for 30 min at 298 K, which was called as solution (A). Then, EtOH (10 mL) was mixed with deionized water (2.5 mL), which was called as solution (B). With the dripping speed of 1 mL min^{-1}, the solution (B) was slowly dripped into the solution (A), which formed light yellow sol, and the yellow sol was treated by the ultrasound for 30 min. As a result, the concentration of 0.0683 g mL^{-1} for N-TiO_2 was successfully obtained, and then it was kept under seal at 298 K.

In this study, the Al_2O_3 ceramic support with a diameter of 52 mm, thickness of 5 mm and pore size of 200 nm was used. It has an effective membrane area of 0.001257 m^2. One side of the ceramic membrane was steeped into N-TiO_2 sol for 5 min, and it was kept for one hour at room temperature. With a heating rate of 2 K min^{-1}, the ceramic membrane was calcined at 723 K for 1 h in N_2 atmosphere, and the N-TiO_2 ceramic membrane was obtained [9]. When the above processes were repeated 7 times, the composite membranes with an average pore size of about 2 nm and pure water flux of 20 L m^{-2} h^{-1} at 0.1 MPa pressure were successfully synthesized. If the coating was repeated more than seven times, the membranes with a pore size of less than 2 nm were obtained due to some of TiO_2 particles plugging membrane pores, and permeation flux decline occurred in experiments. If the coating was repeated less than seven times, the average pore size of membranes was larger than 2 nm, which is not conducive to dye capture. Therefore, the coating was repeated seven times to form the composite membranes employed in this study.

2.3. Experimental set-up

The experimental set-up used in this study is shown in Fig. 1, and it was constructed using a reaction chamber on the right, a separation chamber on the left and a ceramic membrane in the middle. Diaphragm pump with a feed flow of 4 L min^{-1}, transmembrane pressure was regulated by the valve (1) and CF velocity was regulated by the valve (2). Solution pH was adjusted using NaOH or HCl solution. The xenon light was turned on to activate the N-TiO_2 catalyst 10 min later, the experimental set-up started to work.

3. Results and discussion

3.1. Analysis of SEM

SEM images of N-TiO_2 ceramic membranes are shown in Fig. 2. Fig. 2(a) shows that the membrane

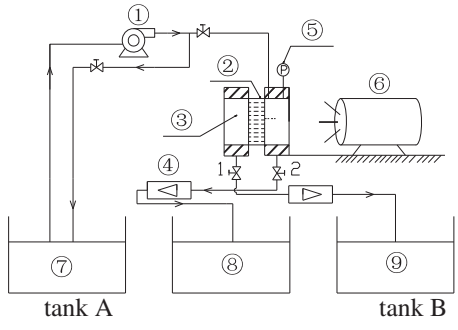

Fig. 1. Experimental set-up used in this study.
Notes: (1) diaphragm pump; (2) ceramic membrane; (3) separation chamber; (4) flow meter; (5) pressure gauge; (6) light; (7) dye-containing aqueous solution; (8) concentrated solution; (9) permeated solution, 1, 2: adjustment valve.

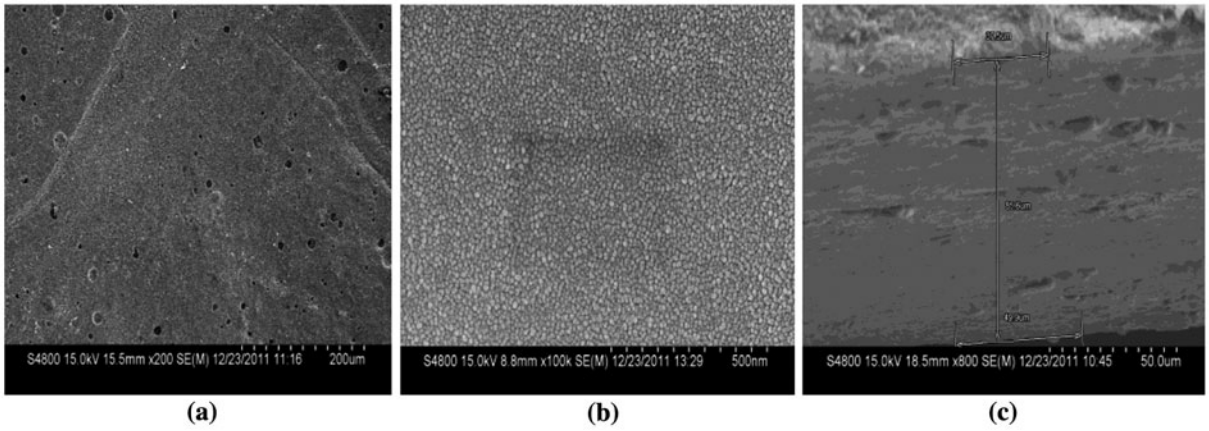

Fig. 2. Surface and section morphology of N-TiO_2 ceramic composite membranes: (a) surface 15.5 mm × 200 SE(M); (b) surface 8.8 × 100 K SE(M); and (c) section 18.5 mm × 800 SE(M).

surfaces were porous and had some defects, which might be the result of non-homogeneous membrane supports. Fig. 2(b) shows that TiO_2 particles of diameter of 7–9 nm were loaded on the ceramic supports to form the composite membranes with an average pore size of about 2 nm. Cross-section of the membranes is shown in Fig. 2(c). As shown in Fig. 2(c), the composite layer became thicker and was still layered because the process for preparation of the composite membranes was repeated seven times.

3.2. Analysis of XRD

XRD patterns of N-TiO_2 composite membranes are shown in Fig. 3. The characteristic peaks at 25.28°, 37.8°, 38.58°, 48.1° and 53.9° are ascribed to the anatase phase of TiO_2. And the characteristic peaks at 36.09°, 41.2°, 62.74° and 69.01° are attributed to the rutile phase of TiO_2. As shown in Fig. 3, there are obvious anatase phases of TiO_2 in the composite membranes, which indicated that amorphous phases of TiO_2 were transformed to anatase phases via calcining composite membranes. According to the calculation from the Scherrer formula ($d = 0.89\,\lambda/\beta\cos\theta$) and XRD patterns, the average diameter of TiO_2 nanocrystals existing in the composites is 8.7 nm. Because of doping N, the crystallinity of TiO_2 sol was affected, and the growth of TiO_2 crystal grains was inhibited. Therefore, the N-doped TiO_2 catalyst has smaller particle size with large surface area [10]. Smaller TiO_2 nanocrystals with a huge surface and an interfacial area can improve their catalytic activities and stability.

The doping of N, the crystal form of TiO_2 was transformed from amorphous phases to anatase, and the percentages of the anatase phases were increased in the mixed crystals. As we all know, anatase phase

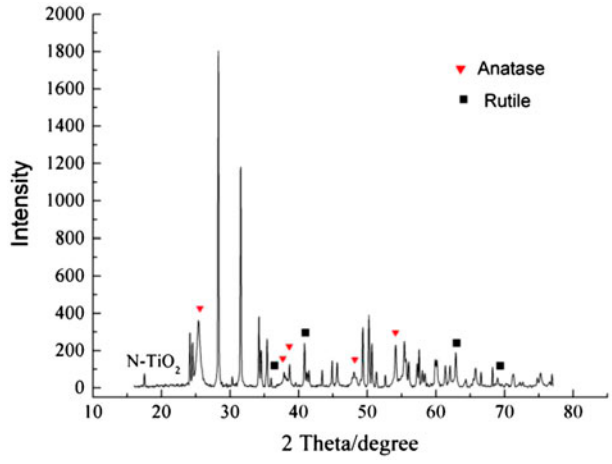

Fig. 3. X-ray diffraction patterns of N-TiO_2 composite membrane.

of TiO_2 in crystals has more defects and dislocations, which generates more oxygen vacancies to improve the activity of photocatalysis reaction [10]. Therefore, it is suggested that the composite membrane synthesized in our work would present a better photocatalytic activity.

3.3. Treatment of dye-containing aqueous solution

3.3.1. Membrane separation and permeation flux

At 293 K using dye concentration of 10 mg L^{-1}, 0.4 MPa transmembrane pressures, zero CF velocity, dye aqueous solution (pH 7) was treated by the N-TiO_2 composite membranes and dye was separated from aqueous solution. The retention rates for dye and membrane flux (permeation flux) are shown in Fig. 4.

Fig. 4(a) shows that the composite membranes had an effect on permeation flux. For the N-TiO_2 nanocrystals, the existence of N inhibited the growth of TiO_2 crystal grains and may refine crystal grains [11,12]. The N-TiO_2 sol with a smaller grain diameter was loaded on the ceramic support to form the N-TiO_2 composite membranes with smaller pore sizes. Therefore, the composite membranes had a lower permeation flux and a higher retention rate for dye in comparison to the undoped TiO_2 ones (Fig. 4(b)). In general, composite membranes with smaller pore sizes have a lower permeation flux to aqueous solution and a higher retention for dye. The experiment results showed that the pore sizes of the N-doped membranes are really smaller than the un-N ones. The N-TiO_2 membranes had a higher retention for dye and the optimum separation property of dye from aqueous solution. Therefore, the N-TiO_2 composite membranes were chosen to work in this study.

In experimentation, the N-TiO_2 composite membranes showed poor working status under visible light. For controlling the membrane fouling, the N-TiO_2 membranes worked under UV light. In lighting (xenon lamp, 300 W, light intensity of 306 Candela and wavelength of 220 nm), the composite membranes had a higher permeation flux in comparison to no light sources, and over 96% permeation flux was obtained (Fig. 4(a)). With the lighting, dye adsorption onto the membrane or within the membrane pores was quickly degraded by photocatalyst (TiO_2 or N-TiO_2), and the temperature was increased in the reaction zone, which also accelerated the mass-transfer rate. The rapid formation of cake layer was prevented, as it was on the concentration polarization [13,14]. Fig. 4(b) shows that the higher retention rate (close to 99%) for dye was obtained in lighting, which indicated that the great amount of dye was captured by the N-TiO_2 membranes. In the photocatalysis, dye on the membrane surfaces was degraded and membrane fouling was effectively inhibited. Therefore, dye within the membrane pores was greatly decreased and the effluent quality was improved. Fig. 4(b) shows that the retention rate of dye using N-TiO_2 membranes was similar to the TiO_2 ones under lighting conditions, but permeation flux decline using N-TiO_2 membrane was gentle in comparison to the TiO_2 membrane (Fig. 4(a)), which indicates that the doping of N in catalyst improves photocatalytic activity [15–17].

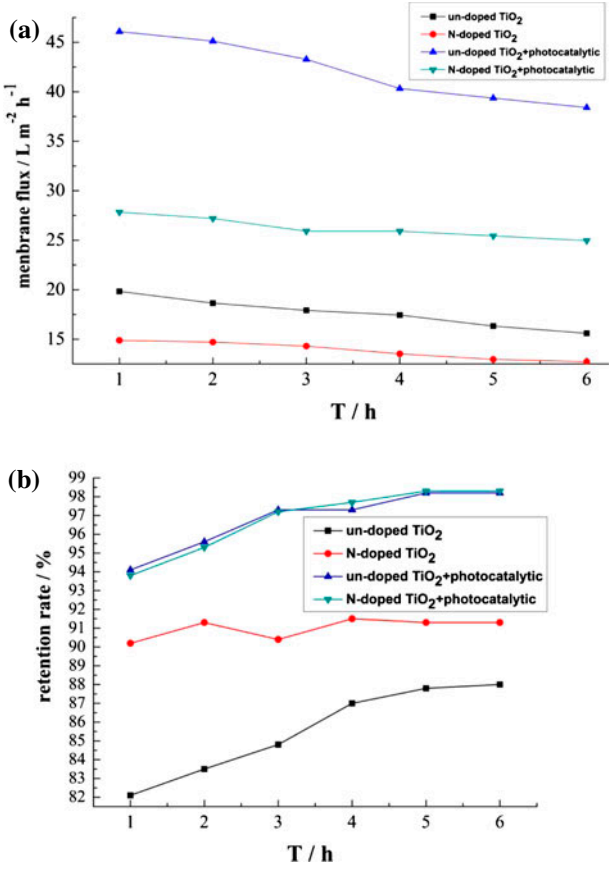

Fig. 4 Effects of composite membrane on (a) membrane flux and (b) retention rate.

3.3.2. Dye concentration

At 293 K using 0.4 MPa transmembrane pressures, zero CF velocity, the dye-containing aqueous solution (pH 7) was treated by the N-TiO_2 composite membranes. The effects of dye concentration on membrane separation and flux are shown in Fig. 5. As shown in Fig. 5(a), the increasing of dye concentration resulted in permeation flux decline. Dye concentration of 10 mg L^{-1}, Fig. 5(a), showed that the optimum flux was obtained. The photocatalytic activity and the permeation flux all decreased with the increasing of the dye concentration. It prevented light irradiation to membrane surface due to the increasing of dye concentration. The higher the dye concentration is, the more quickly the cake layer and the concentration polarization forms. The rapid formation of cake layer and concentration polarization also results in the retention decline for dye. As shown in Fig. 5(b), in the photocatalysis, the N-TiO_2 composite membranes had the lowest retention rate for dye in the dye concentration of 60 mg L^{-1} and did not show the best working status. The most likely reason was that the photocatalytic degradation of dye on the membranes was inhibited, and the membrane fouling might occur in the higher concentration employed. Fig. 5(b) also shows that the retention rates for dye continued to

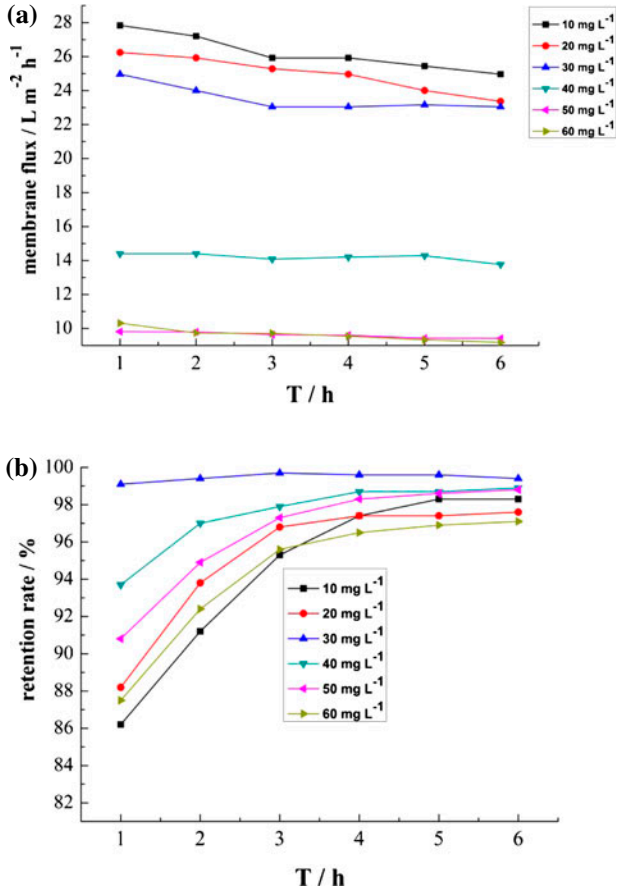

Fig. 5. Effects of dye concentration on (a) membrane flux and (b) retention rate.

rise, and tended to stabilize after 3 h. In the dye concentration of 30 mg L^{-1}, the composite membranes showed the best working status with the retention rate of 99% for dye. However, Fig. 5(b) shows that errors of retention for dye were tiny in the dye concentration range of 30–40 mg L^{-1} after 5 h, and good effluent quality was also obtained in the dye concentration of 40 mg L^{-1}. Therefore, the dye concentration of 40 mg L^{-1} was adopted when the effects of pressure on the flux were investigated. After retention of 6 h, the dye concentration of 0.4 and 39.6 mg L^{-1} were obtained in permeate and retentate solutions, respectively.

3.3.3. Transmembrane pressure

At 293 K using dye concentration of 40 mg L^{-1} (pH 7) and zero CF velocity, the effects of the pressure on permeation flux were investigated at the pressure range of 0.2–0.6 MPa. Pressure plays an important role in the change of flux. Fig. 6 shows that the flux increased with the increasing of pressure at the beginning phase. However, as the pressure continued to increase, the attenuation amplitude of flux also increased. Pressure is the main factor in the formation of cake layer. With the increasing of pressure, dye on the surface of membrane also increased, which lastly accelerated to form the cake layer and resulted in membrane fouling. As shown in Fig. 6, the permeation flux plummeted down when the pressure was higher than 0.4 MPa. However, with 0.4 MPa pressure, the flux remained stationary after 5 h. In order to consume less energy and obtain an optimum flux, the 0.4 MPa pressure was adopted in this study.

3.3.4. CF velocity

In the dye concentration of 10 mg L^{-1}, the optimum permeation flux was obtained (Fig. 5(a)). Therefore, the dye concentration of 10 mg L^{-1} was adopted when the effects of CF velocity on the permeation flux were investigated. At 293 K, 0.4 MPa pressure and solution pH 7, the CF velocity had a great influence on the permeation flux (Fig. 7). CF velocity of less than 300 mL min^{-1}, the flux obviously declined at the beginning phase, and the membranes might be seriously polluted. With CF velocity of 400 mL min^{-1}, the flux slowly declined after 5 h and the composite membranes had an optimum flux, and the concentration polarization was alleviated, which improved the membrane efficiencies lastly. Since the other experiments were studied in the static state test, the zero CF velocity was selected when the effects of pressure, solution pH and dye concentration on membrane separation and flux were investigated.

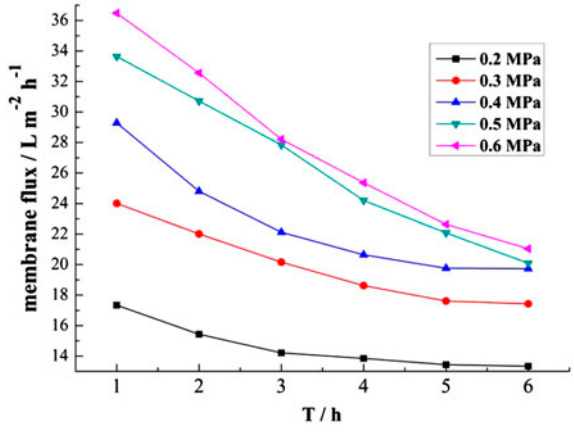

Fig. 6. Effects of pressure on membrane flux.

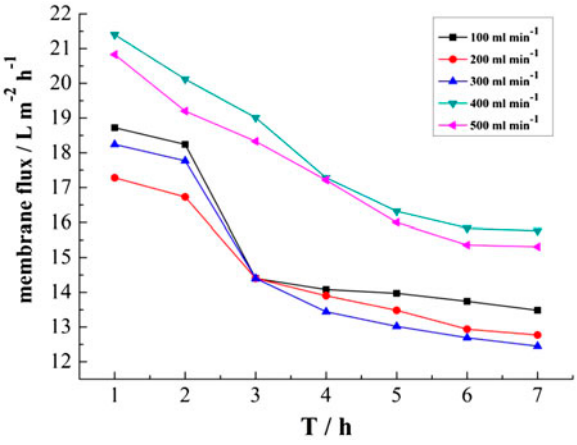

Fig. 7. Effects of CF velocity on membrane flux.

3.3.5. Solution pH

At 293 K using dye concentration of 30 mg L^{-1}, transmembrane pressure of 0.4 MPa and zero CF velocity, pH had no influences on the dye retention. The effects of pH on the flux were studied in the pH range of 1–9. Fig. 8 shows that the composite membranes, in alkaline conditions, had a larger permeation flux. The pH of TiO_2 isoelectric point is 6.3, and the surface of the composite membrane carries negative charge in alkaline conditions, which has an electrostatic repulsion to dye molecules with the negative charges in aqueous solution, and it made membrane pores looser. As a result, the resistance of the composite membranes decreased in solution [18], which might increase permeation flux. In addition, the solution pH also affected the characteristics of dye and photocatalytic products such as protonation or deprotonation, which enhanced the separation efficiencies of photocatalytic products from aqueous solution [19]. Based on the consideration of all factors, the solution pH 7 was adopted in this study.

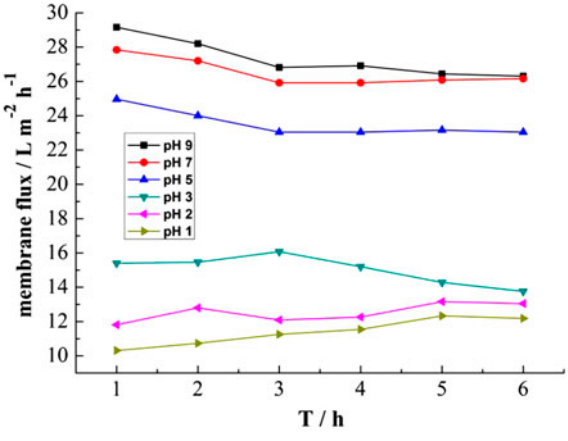

Fig. 8. Effects of pH on membrane flux.

4. Conclusions

The N-TiO_2 sol was loaded on the ceramic membranes for the synthesis of the composite membranes. The composite membrane has an advantage of anti-pollution performance due to the coupling of photocatalysis and membrane separation. This new method would have synergistic effects on the separation of dye from aqueous solution with avoiding membrane fouling. Using 0.4 MPa transmembrane pressure, CF velocity of 400 mL min^{-1} and dye concentration of 30 mg L^{-1} (pH 7), the N-TiO_2 ceramic membranes showed the best working status under lighting conditions and had good stability after reusing several times.

In the paper, artificial dye wastewater studied was only a dye solution. We focused on the effects of photocatalysis on the flux and dye retention. Real dye wastewater, regeneration aspects of the membranes and membrane efficiencies at higher dye concentration will be investigated in future studies.

Acknowledgements

The support from Zhejiang Provincial Technology Application Research Foundation (2011C31031) is highly appreciated.

References

[1] L. Setiawan, R. Wang, K. Li, A.G. Fane, Fabrication of novel poly(amide–imide) forward osmosis hollow fiber membranes with a positively charged nanofiltration-like selective layer, J. Membr. Sci. 369 (2011) 196–205.
[2] M. Turan, Influence of filtration conditions on the performance of nanofiltration and reverse osmosis membranes in dairy wastewater treatment, Desalination 170 (2004) 83–90.
[3] J. Radjenovic´, M. Petrovic´, F. Ventura, D. Barcelo´, Rejection of pharmaceuticals in nanofiltration and reverse osmosis membrane drinking water treatment, Water Res. 42 (2008) 3601–3610.
[4] W.L. Xu, Y. Li, C.L. Yin, R.L. Tu, Inorganic ceramics membrane and application in juice, Agric. Eng. Technol. 7 (2007) 17–20.
[5] B. Van der Bruggen, G. Cornelis, C. Vandecasteele, I. Devreese, Fouling of nanofiltration and ultrafiltration membranes applied for wastewater regeneration in the textile industry, Desalination 175 (2005) 111–119.
[6] A.C. Gomes, I.C. Goncalves, M.N. Pinho, The role of adsorption on nanofiltration of azo dyes, J. Membr. Sci. 255 (2005) 157–165.

[7] J. Ananpattarachai, P. Kajitvichyanukul, S. Seraphin, Visible light absorption ability and photocatalytic oxidation activity of various interstitial N-doped TiO_2 prepared from different nitrogen dopants, J. Hazard. Mater. 168 (2009) 253–261.
[8] Y.M. Wu, M.Y. Xing, B.Z. Tian, J.L. Zhang, F. Chen, Preparation of nitrogen and fluorine co-doped mesoporous TiO_2 microsphere and photodegradation of acid orange 7 under visible light, Chem. Eng. J. 162 (2010) 710–717.
[9] P. Puhlfürß, A. Voigt, R. Weber, M. Morbé, Microporous TiO_2 membranes with a cut off <500 Da, J. Membr. Sci. 174 (2000) 123–133.
[10] L.B. Liao, Q.P. Yang, Preparation and characterization of N-doped nano-TiO_2, Acta Miner. Sin. 28 (2008) 232–235.
[11] L. Han, Y.J. Xin, H.L. Liu, X.X. Ma, G.Z. Tang, Photoelectrocatalytic properties of nitrogen doped TiO_2/Ti photoelectrode prepared by plasma based ion implantation under visible light, J. Hazard. Mater. 175 (2010) 524–531.
[12] Y.X. Li, C.F. Xie, S.Q. Peng, G.X. Lu, S.B. Li, Eosin Y-sensitized nitrogen-doped TiO_2 for efficient visible light photocatalytic hydrogen evolution, J. Mol. Catal. A: Chem. 282 (2008) 117–123.
[13] Y.T. Xiao, S.S. Xu, Z.H. Li, X.H. An, L. Zhou, Y.L. Hang, Q.S. Fu, Progress of applied research on TiO_2 photocatalysis-membrane separation coupling technology in water and wastewater treatment, Chin. Sci. Bull. 55 (2010) 1085–1093.
[14] S. Hong, M. Elimelech, Chemical and physical aspects of natural organic matter (NOM) fouling of nanofiltration membranes, J. Membr. Sci. 132 (1997) 159–181.
[15] F. Dong, W.R. Zhao, Z.B. Wu, S. Guo, Band structure and visible light photocatalytic activity of multi-type nitrogen doped TiO_2 nanoparticles prepared by thermal decomposition, J. Hazard. Mater. 162 (2009) 763–770.
[16] M. Chekini, M.R. Mohammadizadeh, S.M. Vaez Allaei, Photocatalytic and superhydrophilicity properties of N-doped TiO_2 nanothin films, Appl. Surf. Sci. 257 (2011) 7179–7183.
[17] J. Senthilnathan, L. Philip, Photocatalytic degradation of linden under UV and visible light using N-doped TiO_2, Chem. Eng. J. 161 (2010) 83–92.
[18] S.H. Fan, Z.F. Sun, Q.Z. Wu, Y.G. Li, Adsorption and photocatalytic kinetics of azo dyes, Acta Phys-Chim. Sin. 19 (2003) 25–29.
[19] L.M. Liu, J.L. Chen, Q.L. Gao, Y.J. Yang, K. Qi, Photocatalytic degradation of 4BS dyestuff over TiO_2/SiO_2, Ind. Catal. 17 (2009) 71–74.